IMPLEMENTATION OF LOW-POWER GNSS AND GEOMAGNETICS POSITIONING ON SINGLE BOARD COMPUTER

Kouki Kurita, Sho Sanuka, Masafumi Nakagawa

Shibaura Institute of Technology,
3-7-5, Toyosu, Koto-ku, Tokyo 135-8548, Japan

E-mail: ah16206@shibaura-it.ac.jp; ah16028@shibaura-it.ac.jp; mnaka@shibaura-it.ac.jp

ABSTRACT: GNSS positioning is hard to be used in indoor environments. Thus, many indoor positioning approaches have been developed, such as Wi-Fi positioning, Beacon positioning, IMES positioning, visible light positioning, and geomagnetic positioning. Moreover, indoor-outdoor seamless positioning approach is also discussed for location-based services in urban areas. However, there are various technical issues, such as positioning accuracy, device cost, and smooth positioning mode switching between outdoor and indoor environments. In this study, we proposed an indoor-outdoor seamless positioning methodology with single-frequency GNSS single positioning and fingerprint-based geomagnetic positioning. In our experiments, we implemented a low-cost and low-power GNSS receiver and geomagnetic sensor on a single board computer. Through our experiments, our methodology can achieve positioning among indoor and outdoor environments.

1. INTRODUCTION

Various systems and services using location-based services (LBS) have been developed in various fields (Liu et al., 2007). In recent years, many navigation satellites have been launched to improve the availability and continuity of independent positioning in outdoor space. On the other hand, although Wi-Fi (Ren et al., 2019) (Chang et al., 2010), beacon (Arai et al., 2019), indoor messaging systems (IMES), and visible light positioning have been developed, there remain technical issues of positioning system integration in both cost and accuracy. Moreover, because the outdoor positioning differs from indoor positioning, it is necessary to switch the positioning mode according to the environment. However, indoor-outdoor seamless positioning has been discussed about smooth switching between indoor and outdoor positioning modes (Pei et al., 2009) (Zhu, et al., 2019). In this study, we focus on low-cost mobile devices, such as power-saving GNSS receivers, geomagnetic sensors, and single-board computers, to propose a methodology for indoor-outdoor seamless positioning.

2. METHODOLOGY

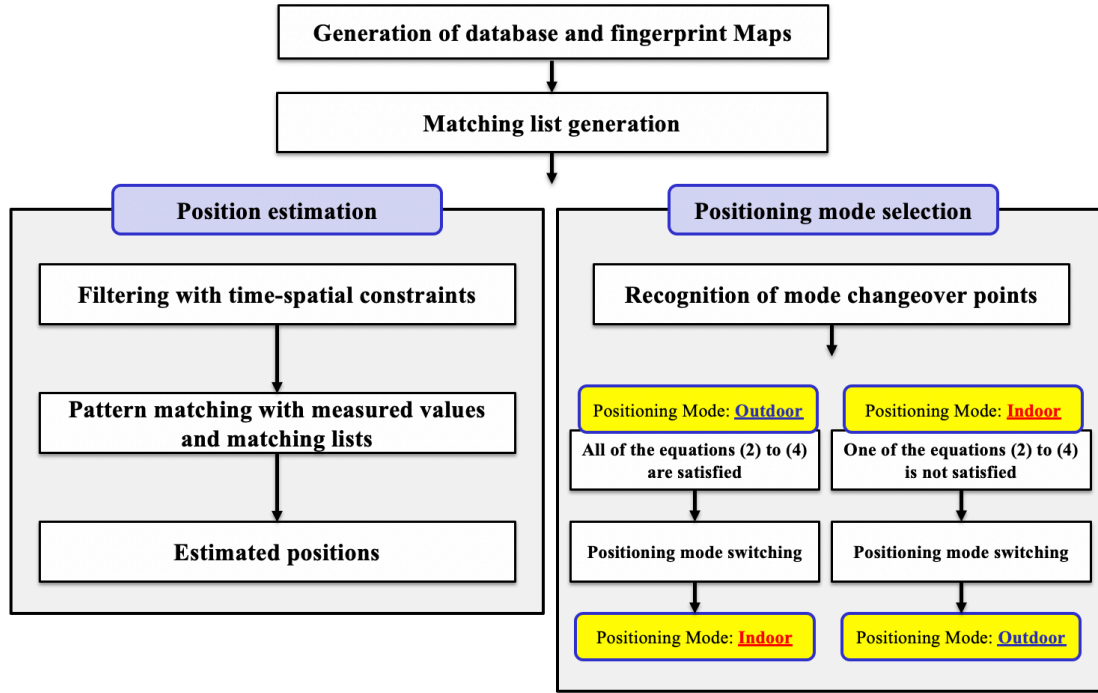Our proposed methodology is shown in Figure 1.

Figure 1. Proposed methodology

2.1 iBeacon positioning and ranging

Ranging-based beacon positioning is based on RSSI values of beacons, such as iBeacon. In ranging using RSSI values, a distance between the transmitter and receiver is estimated based on the Friis transfer formula (1) (Chang et al., 2010 and Arai et al., 2019).

$$RSSI = TxPower - 10n \times \log d \bullet\bullet\bullet(1)$$

TxPower: RSSI value at 1 m between transmitter and receiver

d: Distance between transmitter and receiver n: damping ratio

2.2 RSSI-based positioning using geomagnetic data

We applied multi-GNSS single positioning for outdoor positioning, and we applied received signal strength indicator (RSSI)-based positioning using fingerprint maps generated from geomagnetic data for indoor positioning (Pei et al., 2009). In the RSSI-based positioning, a fingerprint map is firstly generated using previously measured 3D geomagnetic data; M_xn, M_yn, and M_zn. In the fingerprint map generation, a matching list is generated using 3D geomagnetic data measured at grid points with equal intervals in advance. After the fingerprint map generation, a pattern matching is applied for positioning using the fingerprint map and acquired geomagnetic data (P_xn, P_yn, and P_zn) based on the following questions from (2) to (4) as constraints. Then, a matching list is used for positioning with thresholds, such as T_xn, T_yn, and T_zn, to correspond with measured 3D magnetic data in pattern matching for position estimation. We add a threshold value A to improve the stability of pattern matching. We also imposed constraints on time and space to eliminate failed positional estimates that indicate an impossible movement in time and space. When all constraints are satisfied, the positioning mode is switched from outdoor positioning to indoor positioning. Otherwise, the positioning mode is switched from indoor positioning to outdoor positioning.

$$P_{xn} \lessgtr M_{xn} \pm A = T_{xn} \bullet\bullet\bullet(2)$$
$$P_{yn} \lessgtr M_{yn} \pm A = T_{yn} \bullet\bullet\bullet(3)$$
$$P_{zn} \lessgtr M_{zn} \pm A = T_{zn} \bullet\bullet\bullet(4)$$

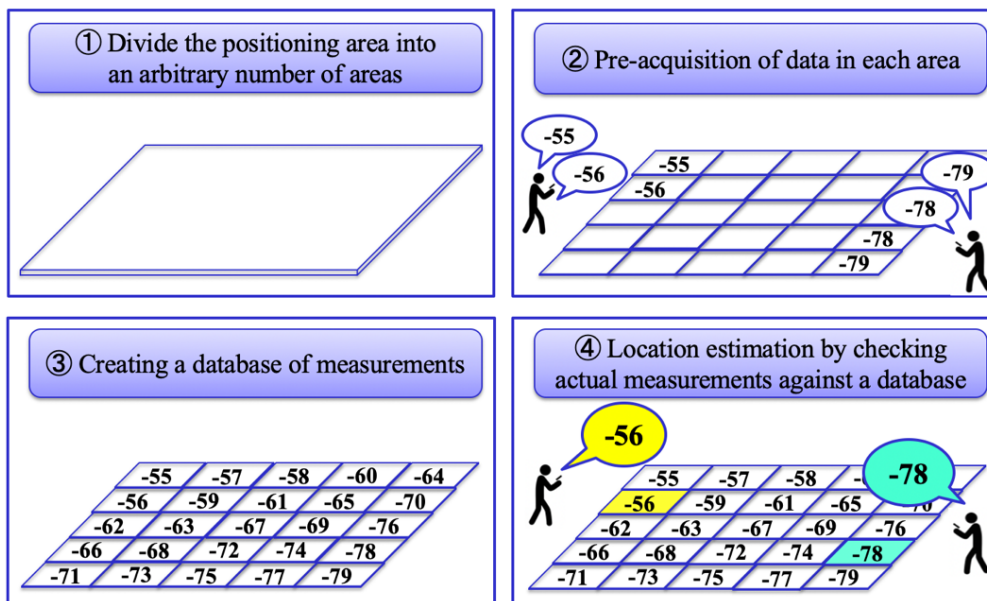Figure 2. RSSI positioning using fingerprint map

3. EXPERIMENTS

In this study, Spresense (SONY) was selected as a single-board computer (Figure 3), and the power-saving GNSS receiver processor (CXD5602, SONY) on Spresense was used for GNSS positioning. The add-on board (Spresense-SENSOR-EVK-701, ROHM) was installed with 1422AGMV and 1422AGMV (ROHM) to enable geomagnetic positioning. Geomagnetic data were acquired at 12 positions in advance. Moreover, GNSS positioning and geomagnetic data were simultaneously acquired using Spresense with walking between indoor and outdoor spaces.

3.1 Preliminary experiment on stability evaluation

An experiment was conducted to evaluate iBeacon ranging using received signals at a fixed point (180 seconds x 10 units). The distance between the transmitter and receiver was calculated using the strength of radio reception and the Friis transfer formula (1), and the difference between the maximum and minimum values was evaluated. We used a note PC (MacBook Air) as a receiver and iBeacon devices (MyBeacon MB004Ac, Aplix) as transmitters. Each equipment was respectively installed at 70 cm height from a floor, with distances between the transmitter and receiver from 1 m to 5 m. In iBeacon ranging, we used the Node.js bleacon library. In this experiment, Spresense was connected to a laptop PC (Surface Pro), and three fixed-point observations of the geomagnetic data were carried out for 180 seconds at three arbitrary locations, and the variability of the data was evaluated (Figure 4).
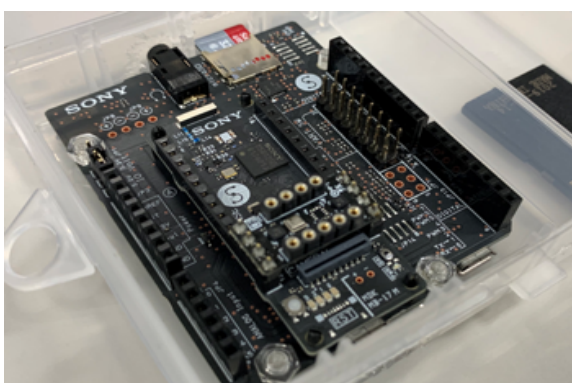

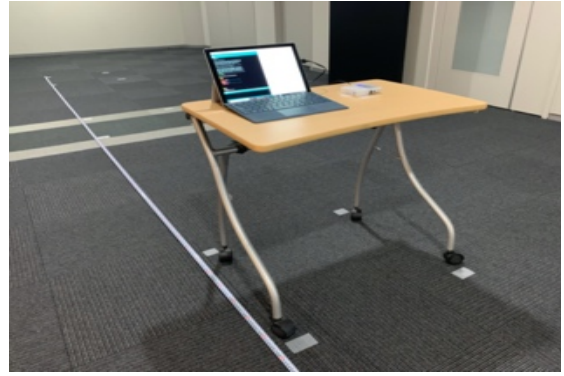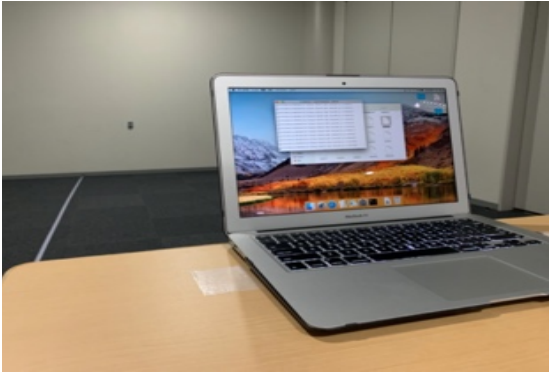Figure 3. Used devices (left: Spresense, and right: MyBeacon)

Figure 4. Preliminary experiments in indoor environments
(left: iBeacon positioning, and right: geomagnetic positioning)

3.2 Indoor-outdoor seamless positioning

Based on the preliminary experiment of iBeacon ranging and geomagnetic, we applied geomagnetic positioning as higher stable indoor positioning. Geomagnetic data were measured in advance at 12 positions in both indoor and outdoor spaces, and Spresense was used to measure the geomagnetic data with multi-GNSS single positioning data simultaneously.
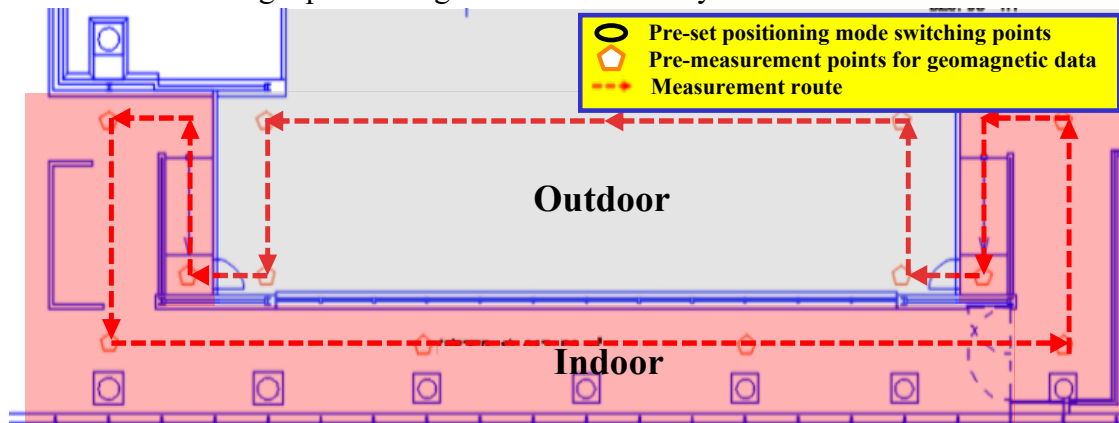

Figure 5. Waypoints and paths in premeasurement

4. RESULTS

4.1 Results of stability evaluation of iBeacon ranging and geomagnetic positioning

Figure 6 and Table 1 show a part of the stability evaluation results of iBeacon ranging. In Figure 6, the vertical axis is the RSSI (Received Signal Strength Indicator) [dBm] and the horizontal axis is the measurement time [s].
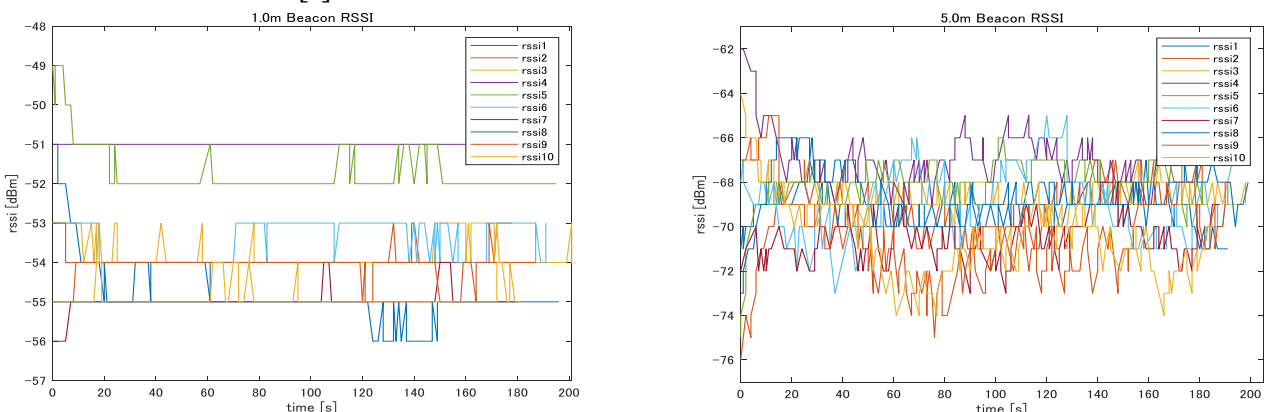

Figure 6. Fixed-point observation of RSSI values (left: 1m, and right: 5m)

Table 1. Variances and standard deviations of
Fixed-point observations of radio reception intensity for each individual

Distance between transmitter and receiver 1.0m										
Individual number	1	2	3	4	5	6	7	8	9	10
Variance	0.268	0.129	0.168	0.006	0.389	0.237	0.080	0.100	0.103	0.088
Standard deviation	0.518	0.359	0.410	0.075	0.624	0.487	0.283	0.316	0.321	0.297
Distance between transmitter and receiver 5.0m										
Individual number	1	2	3	4	5	6	7	8	9	10
Variance	0.611	2.311	0.507	1.635	1.373	2.510	1.074	1.453	3.933	3.115
Standard deviation	0.782	1.520	0.712	1.279	1.172	1.584	1.037	1.206	1.983	1.765

Figures 7, 8, and 9 show a part of the stability evaluation results of geomagnetic positioning. In Figures 7, 8, and 9, the vertical axis is the magnetic flux density $[\mu T]$ and the horizontal axis is the measurement time [s]. Table 2 also shows a part of the stability evaluation results of geomagnetic positioning related to variance and standard deviation of fixed-point observations of geomagnetic data.
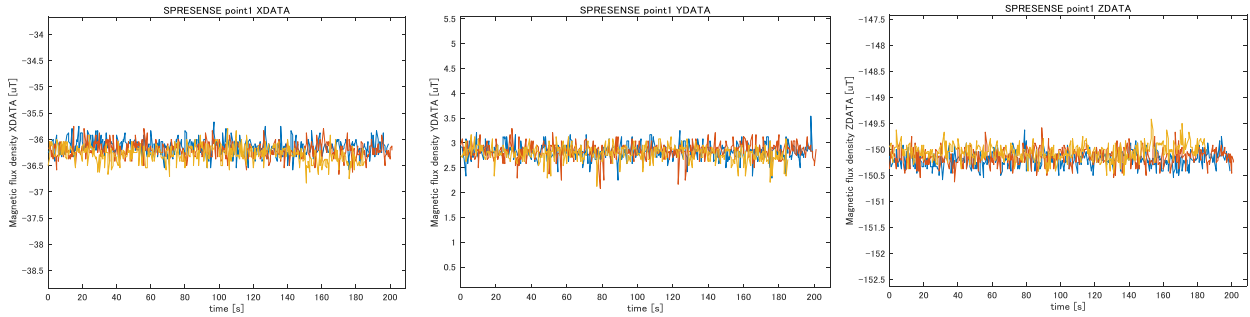

Figure 7. Results of fixed-point geomagnetic observation at
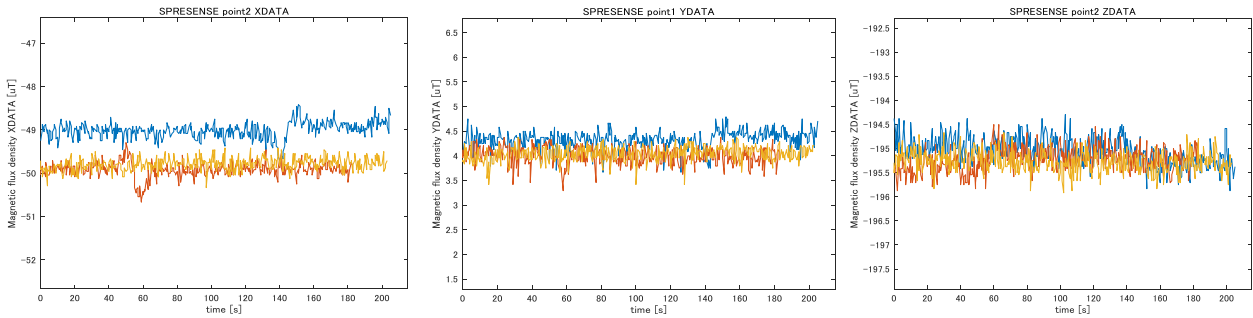Point 1 (left: X-axis, center: Y-axis, and right: Z-axis)

Figure 8. Results of fixed-point geomagnetic observation at
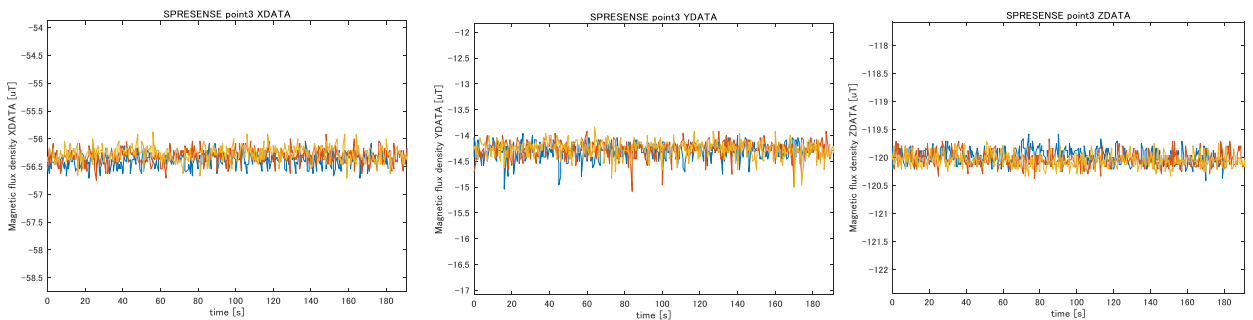Point 2 (left: X-axis, center: Y-axis, and right: Z-axis)

Figure 9. Results of fixed-point geomagnetic observation at
Point 3 (left: X-axis, center: Y-axis, and right: Z-axis)

Table 2. Variance and standard deviation of fixed-point observations of geomagnetic data

Geomagnetic data Point 1								
Number of measurements	1			2			3		
Type of data	XDATA	YDATA	ZDATA	XDATA	YDATA	ZDATA	XDATA	YDATA	ZDATA
Variance	0.024	0.025	0.022	0.021	0.025	0.025	0.027	0.025	0.027
Standard deviation	0.156	0.157	0.149	0.144	0.158	0.157	0.164	0.157	0.164
Geomagnetic data Point 2								
Number of measurements	1			2			3		
Type of data	XDATA	YDATA	ZDATA	XDATA	YDATA	ZDATA	XDATA	YDATA	ZDATA
Variance	0.036	0.032	0.083	0.032	0.031	0.061	0.022	0.024	0.048
Standard deviation	0.191	0.179	0.287	0.178	0.177	0.248	0.149	0.154	0.219
Geomagnetic data Point 3								
Number of measurements	1			2			3		
Type of data	XDATA	YDATA	ZDATA	XDATA	YDATA	ZDATA	XDATA	YDATA	ZDATA
Variance	0.016	0.025	0.018	0.016	0.026	0.017	0.018	0.025	0.014
Standard deviation	0.127	0.158	0.134	0.128	0.160	0.131	0.134	0.157	0.120

In iBeacon ranging, the maximum temporal variation of RSSI values was 4 [dBm] at 1 m and 10 [dBm] at 5 m. The maximum distance difference of 190 m between the transmitter and receiver at 5 m was measured. The total geomagnetic data converged to about approximately 1.0 [μT] in 180 seconds.

4.2 Indoor-outdoor seamless positioning results

Figure 10 shows indoor-outdoor seamless positioning results. The light blue dotted line shows the actual measurement route. The solid blue line shows outdoor positioning mode and the solid red line shows indoor positioning mode. The black dots are positions recorded at points switched from outdoor to indoor positioning mode, and the pink dots are the positions recorded at switched from indoor to outdoor positioning mode. The star mark indicates the actual position switched from indoor to outdoor positioning mode.
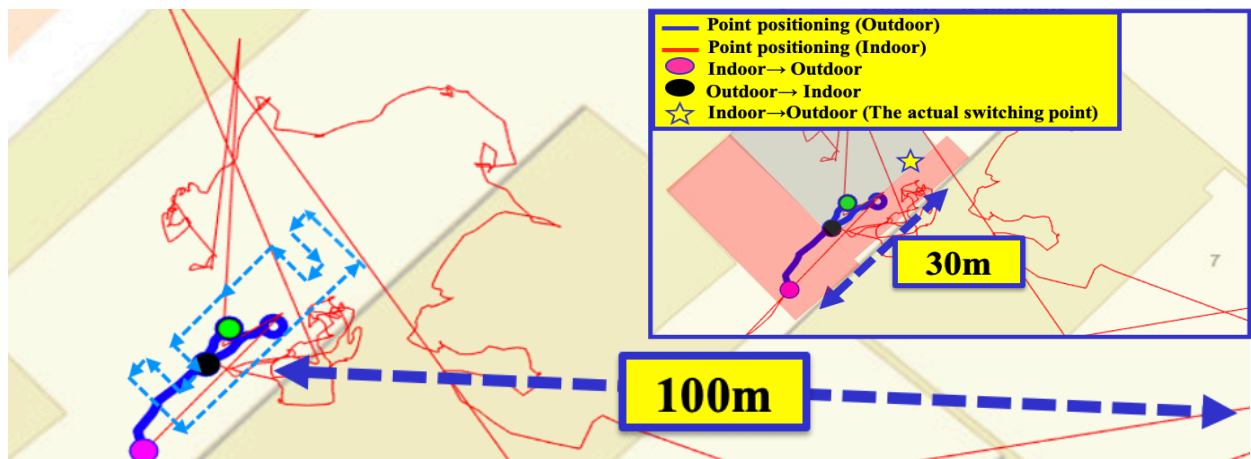

Figure 10. Results of seamless indoor-outdoor positioning

5. DISUCUSSION

5.1 Stability evaluation of iBeacon ranging and geomagnetic positioning

Figure 6 and Table 1 show that as the distance between the transmitter and receiver increases, the variation in radio reception intensity increases, resulting in a larger iBeacon ranging error. However, since this experiment deals with experimental data only when the iBeacon is installed at 70 cm height from the floor, we need to discuss more from the results of multiple patterns of iBeacon placement

at different heights. Table2 shows that the geomagnetic survey is a more stable indoor positioning methodology, since stable data were obtained from fixed-point observations. The reason why the positional estimation is nearly accurate in geomagnetic positioning by fingerprinting based on geomagnetic data is shown in Figure 11, which is a fingerprint map of the X-, Y-, and Z-axes, respectively. In the Fingerprint method, if there is not much difference between the measurements in each region, there is a high probability of incorrect position estimation. However, in this study, we increase the conditions for estimating a particular position by dealing with the X-, Y-, and Z-axes and imposing constraints on time and space to avoid incorrect position estimation.
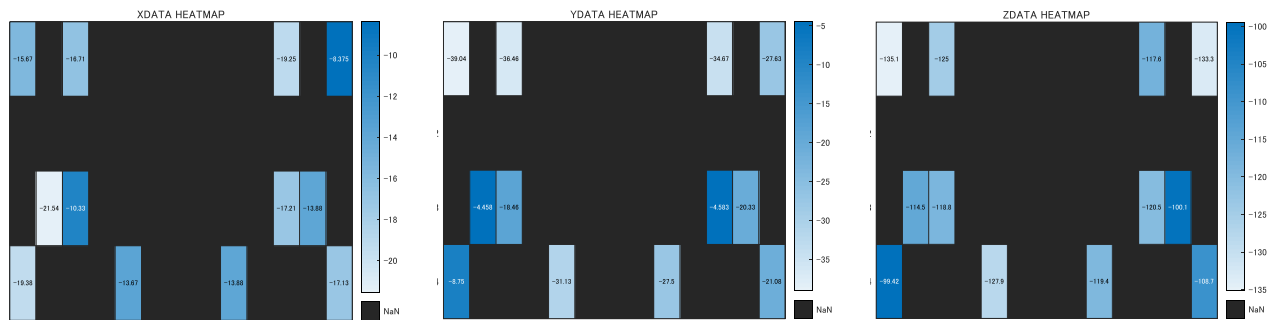

Figure 11 Fingerprint maps for RSSI-based positioning

5.2 Indoor-outdoor seamless positioning

We verified that a power-saving GNSS receiver can acquire precise position data. We also confirmed that our methodology can estimate the positions with a geomagnetic sensor. Moreover, we confirmed that our methodology can change the positioning mode from outdoor to indoor positioning mode using the status of GNSS positioning accuracy. We also confirmed that our methodology can select the positioning mode from indoor to outdoor mode. However, results include approximately 30 m errors from tactual switching points, because the positioning mode was switched from geomagnetic positioning to GNSS positioning under the poor GNSS positioning environments. In this study, although we used geomagnetic data for the positioning mode selection, the performance of positioning mode selection can be improved with additional information, such as GPS time, the number of visible satellites, and dilution of precision (DOP).

6. CONCLUSION

In this study, we selected an indoor positioning methodology with high stability based on two evaluations of indoor positioning methods: iBeacon positioning and ranging and geomagnetic positioning and proposed an indoor-outdoor seamless positioning methodology combined with GNSS independent positioning. For indoor positioning, a fingerprint methodology based on geomagnetic data is used. In order to switch between outdoor and indoor positioning modes, we set the threshold value by adding an adjustment value that takes into account the temporal variation of the geomagnetic data to the most frequent value of the geomagnetic data for creating fingerprint maps. We also applied constraints on time and space to eliminate failed positional estimates that indicate an impossible movement in real spaces. We confirmed that our approach can be used for indoor-outdoor positioning with low-cost devices.

Future issues are to improve the efficiency of pre-generating Fingerprint maps and to reduce the computation time of GNSS positioning when moving from indoor spaces or spaces where GNSS positioning cannot be performed accurately to outdoor spaces. In addition, we would like to carry out verification using RTK-GNSS positioning as well as multi-GNSS single positioning.

References from Journals:
Arai Taiga, Yoshizawa Takahiro, Aoki Takuya, Zempo Keiichi, Okada Yukihiko, 2019, Evaluation of Indoor Positioning System based on Attachable Infrared Beacons in Metal Shelf Environment, Proceeding of the 37th IEEE International Conference on Consumer Electronics, pp. 1-4.

Hui Liu, Houshang Darabi, Pat Banerjee, Jing Liu, 2007, Survey of Wireless Indoor Positioning Techniques and Systems, IEEE Transactions on Systems, Man, and Cybernetics, Part C, Applications and Reviews Volume: 37, Issue: 6, pp. 1067-1080.

Ning Chang, Rashid Rashidzadeh, Majid Ahmadi 2010. Robust Indoor Positioning using Differential Wi-Fi Access Points, IEEE Transactions on Consumer Electronics, Vol. 56, No. 3, pp. 1860-1867.

References from Other Literature:
Jingqiu Ren, Ke Bao, Siyue Sun, Weidang Lu, 2019. Research on Indoor and Outdoor Seamless Positioning Based on Combination of Clustering and GPS. AICON2019 pp. 225-239.

Ling Pei, Ruizhi Chen, Yuewei Chen, Helena Leppäkoski, Arto Perttula, 2009, Indoor/Outdoor Seamless Positioning Technologies Integrated on Smart Phone, 2009 First International Conference on Advances in Satellite and Space Communications, Colmar, 2009, pp. 141-145.

Ni Zhu, Miguel Ortiz, Valérie Renaudin, 2019. Seamless Indoor-Outdoor Infrastructure-free Navigation for Pedestrians and Vehicles with GNSS-aided Foot-mounted IMU, International Conference on Indoor Positioning and Indoor Navigation (IPIN), pp. 1-8.